The Alveolar Epithelium Determines Susceptibility to Lung Fibrosis in Hermansky-Pudlak Syndrome

Lisa R. Young[1,2], Peter M. Gulleman[1], James P. Bridges[3], Timothy E. Weaver[3], Gail H. Deutsch[4], Timothy S. Blackwell[2], and Francis X. McCormack[5]

[1]Division of Pulmonary Medicine, Department of Pediatrics, and [2]Division of Allergy, Pulmonary, and Critical Care Medicine, Department of Medicine, Vanderbilt University School of Medicine, Nashville, Tennessee; [3]Division of Pulmonary Biology, Cincinnati Children's Hospital Medical Center, Cincinnati, Ohio; [4]Department of Pathology, Seattle Children's Hospital, Seattle, Washington; and [5]Division of Pulmonary, Critical Care, and Sleep Medicine, Department of Medicine, The University of Cincinnati College of Medicine, Cincinnati, Ohio

***Rationale*: Hermansky-Pudlak syndrome (HPS) is a family of recessive disorders of intracellular trafficking defects that are associated with highly penetrant pulmonary fibrosis. Naturally occurring HPS mice reliably model important features of the human disease, including constitutive alveolar macrophage activation and susceptibility to profibrotic stimuli.**

***Objectives*: To decipher which cell lineage(s) in the alveolar compartment is the predominant driver of fibrotic susceptibility in HPS.**

***Methods*: We used five different HPS and Chediak-Higashi mouse models to evaluate genotype-specific fibrotic susceptibility. To determine whether intrinsic defects in HPS alveolar macrophages cause fibrotic susceptibility, we generated bone marrow chimeras in HPS and wild-type mice. To directly test the contribution of the pulmonary epithelium, we developed a transgenic model with epithelial-specific correction of the HPS2 defect in an HPS mouse model.**

***Measurements and Main Results*: Bone marrow transplantation experiments demonstrated that both constitutive alveolar macrophage activation and increased susceptibility to bleomycin-induced fibrosis were conferred by the genotype of the lung epithelium, rather than that of the bone marrow–derived, cellular compartment. Furthermore, transgenic epithelial-specific correction of the HPS defect significantly attenuated bleomycin-induced alveolar epithelial apoptosis, fibrotic susceptibility, and macrophage activation. Type II cell apoptosis was genotype specific, caspase dependent, and correlated with the degree of fibrotic susceptibility.**

***Conclusions*: We conclude that pulmonary fibrosis in naturally occurring HPS mice is driven by intracellular trafficking defects that lower the threshold for pulmonary epithelial apoptosis. Our findings demonstrate a pivotal role for the alveolar epithelium in the maintenance of alveolar homeostasis and regulation of alveolar macrophage activation.**

AT A GLANCE COMMENTARY

Scientific Knowledge on the Subject

Hermansky-Pudlak syndrome (HPS) is a highly penetrant genetic disorder of pulmonary fibrosis, and there is strong evidence that macrophage-mediated inflammation precedes pulmonary fibrosis in patients with HPS. The spontaneous development of fibrosis in the HPS murine model recapitulates important features of the human disease, including constitutive alveolar macrophage activation and genotype-specific susceptibility to profibrotic stimuli.

What This Study Adds to the Field

Constitutive alveolar macrophage activation and increased susceptibility to bleomycin-induced fibrosis are attributable to HPS mutations in the alveolar epithelium. These findings demonstrate a pivotal role for the epithelium in the maintenance of alveolar homeostasis and regulation of alveolar macrophage activation and have implications for both for patients with Hermansky-Pudlak syndrome and for those with fibrotic lung diseases from other causes.

Keywords: lung fibrosis; alveolar epithelial cells; alveolar macrophage; Hermansky-Pudlak syndrome; adaptor protein 3

Pulmonary fibrosis is a final common pathway in many forms of interstitial lung diseases (ILD). Inflammation plays a prominent role in some forms of ILD and is a driver of fibrosis in other organs. However, idiopathic pulmonary fibrosis (IPF), the most common and enigmatic form of lethal pulmonary fibrosis in adults, does not respond to antiinflammatory therapies. Currently, the development of preventative and therapeutic strategies remains limited by incomplete understanding of the mechanisms underlying alveolar fibrosis (1).

Hermansky-Pudlak syndrome (HPS), the most penetrant of the genetic pulmonary fibrosis syndromes, provides a compelling paradigm for studying the cellular pathogenesis of pulmonary fibrosis. HPS gene products are ubiquitously expressed, and recessive mutations result in defects in heterooligomeric intracellular protein trafficking complexes and oculocutaneous albinism, bleeding diathesis, and sometimes granulomatous colitis (2). There are currently nine genetic loci associated with HPS in humans, and pulmonary fibrosis has been associated with some but not all genotypes, including HPS-1 and HPS-2 (2–6). Lung histology from patients with HPS typically reveals the usual interstitial pneumonia pattern found in IPF (7).

The alveolus is composed of and inhabited by numerous cell types, most of which have been extensively studied in efforts to understand the pathogenesis of pulmonary fibrosis. Both alveolar macrophages (8–13) and alveolar epithelial cells (14–17) have been

(*Received in original form July 12, 2012; accepted in final form September 10, 2012*)

Funded by the American Thoracic Society/Hermansky-Pudlak Syndrome Network Partnership Grant (L.R.Y.); Parker B. Francis Foundation Fellowship (L.R.Y.); National Institutes of Health grants K08 HL082757 (L.R.Y.), HL85317 (T.S.B.), HL92870 (T.S.B.), and HL68861 (F.X.M.); and the Department of Veterans Affairs (T.S.B. and F.X.M.).

Author Contributions: L.R.Y. was responsible for the overall project and wrote the initial manuscript. P.M.G. performed the majority of the animal and cell culture experiments. T.E.W. was responsible for generation of the transgenic construct. J.P.B. contributed to the design and conduct of the endoplasmic reticulum stress experiments. G.H.D. performed electron microscopy analysis. T.S.B. contributed to the data analysis and manuscript preparations. F.X.M. contributed to the overall project inception, experimental design, data analysis, and execution. All authors edited the manuscript.

Correspondence and requests for reprints should be addressed to Lisa R. Young, M.D., Division of Pulmonary Medicine, Department of Pediatrics, Vanderbilt University School of Medicine, 2200 Children's Way, 11215 Doctor's Office Tower, Nashville, TN 37232. E-mail: Lisa.Young@vanderbilt.edu

This article has an online supplement, which is accessible from this issue's table of contents at www.atsjournals.org

Am J Respir Crit Care Med Vol 186, Iss. 10, pp 1014–1024, Nov 15, 2012

Originally Published in Press as DOI: 10.1164/rccm.201207-1206OC on October 4, 2012
Internet address: www.atsjournals.org

implicated in the pathogenesis of fibrosis in humans and experimental models, including in HPS (18–23), although the causal relationships have remained unknown. Type II cell hyperplasia and endoplasmic reticulum (ER) stress have been identified in end-stage HPS lung disease (23). However, there is strong evidence that macrophage-mediated inflammation precedes pulmonary fibrosis in patients with HPS, and based on these data, bone marrow transplantation has been proposed as a potential therapy (19).

Naturally occurring HPS mouse models share many features of the human disease, but spontaneous pulmonary fibrosis does not occur (24). However, HPS-1 mice have an exaggerated fibrotic response to silica (25), and both the HPS-1 and HPS-2 models are exquisitely susceptible to bleomycin-induced fibrosis (18). Recent reports of spontaneous fibrosis in an HPS double-mutant mouse, generated by mating the HPS-1 and HPS-2 mutant mice, support the use of HPS models to study pulmonary fibrosis (21, 23). The gene product of *HPS2* in mice and humans is the β3A subunit of the Adaptor Protein-3 (AP-3) complex, a heterooligomer that functions in organelle biogenesis and protein trafficking (26, 27). Mutations in individual AP-3 subunits result in instability and ubiquitin-mediated degradation of the entire AP-3 complex (26, 28), and loss of AP-3 function leads to protein mistrafficking in a variety of cell types (29). Both HPS-1 and HPS-2 mutant mice exhibit alveolar macrophage activation and fibrotic susceptibility and therefore provide a platform to experimentally model human HPS disease (18, 20). We therefore used cell-specific genetic correction and cellular replacement to decipher which cell lineage(s) in the alveolar compartment is the predominant driver of HPS fibrotic susceptibility. Some results have been previously reported in abstract form (30–32).

METHODS

Mice

Table 1 details the HPS mouse models studied and the corresponding disease-causing human HPS genotypes. Mice with homozygous mutations (hereafter by genotype and mutant [*mt*] or knock-out [*ko*]) on the C57BL/6J background were used in these studies (24, 27, 33, 34). The online supplement details the source of models used. Mice were housed in a barrier facility and studied using procedures approved by the Institutional Animal Care and Use Committees at the University of Cincinnati, Cincinnati Children's Hospital Medical Center, and Vanderbilt University.

Bleomycin Challenge

Pharmaceutical grade bleomycin sulfate (0.025 units) was administered by intratracheal instillation (18).

Quantitation of Lung Collagen Content

Whole lung total soluble collagen was measured using the Sircol assay (Biocolor; Accurate Chemical and Scientific Corporation, Westburg, NY).

Lung Histology, Immunohistochemistry, and Evaluation of Apoptosis

Lung tissues were prepared and studied as described in the online supplement. Terminal deoxynucleotidyl transferase-mediated dUTP nick end labeling (TUNEL) was performed using the In Situ Cell Death Detection Kit (Roche Diagnostics, Mannheim, Germany).

Isolation of Murine Alveolar Macrophages and Type II Cells

Alveolar macrophages were isolated as previously described (20). Type II cells were isolated using Dispase and negative selection on antibody-coated plates to separate leukocyte and monocyte populations (35). Detailed methods and culture conditions are provided in the online supplement. Cytokine levels were measured in the cell culture media supernatant by ELISA (R&D Systems, Minneapolis, MN). Cytotoxicity was determined using an lactate dehydrogenase (LDH) assay (Promega, Madison, WI).

Quantitative Real-Time Polymerase Chain Reaction Analysis and Western Blot Analysis

Total RNA for quantitative polymerase chain reaction was isolated and reverse transcribed by standard methods, with quantification on an Applied Biosystems Step One Plus Cycler. Primer probe sequences and Western blot protocols and antibody information are provided in the online supplement.

Bone Marrow Transplantation

Recipient mice were exposed to split dose whole body irradiation of 7 Gy then 4.75 Gy followed by tail vein injection of whole marrow, as described in the online supplement. To facilitate identification of donor versus recipient cell populations, we used C57BL/6J mice, which express green fluorescent protein under the direction of the human ubiquitin C promoter (WT-GFP), as wild-type control mice and donor mice in some experiments.

Epithelial-Specific Transgenic Correction of AP-3 in HPS Mice

The cDNA for the murine *HPS2* gene product, AP-3/β3A, was fully sequenced, and a construct was generated with the following elements (in order): human SPC promoter (3.7 kb), β globin sequence, AP3 (3.4 kb), and polyadenylation signal. This construct was linearized and injected into the pronuclei of fertilized mouse C57BL/6J embryos and implanted into pseudopregnant C57BL/6J dams. Founders were crossed with HPS2 mice as detailed in the online supplement.

Statistical Analysis

Numeric data are presented as mean ± SEM. Statistical analyses were performed using GraphPad Prism. Parametric data were evaluated by analysis of variance with Tukey *post hoc* analysis, nonparametric data by the Mann-Whitney test, and survival analysis using the log-rank test. A two-sided probability value less than 0.05 was regarded as significant.

RESULTS

Susceptibility to Bleomycin-induced Fibrosis Occurs Only in Those Mouse Models with HPS Mutations Corresponding to Human Genotypes Associated with Lung Disease

ILD has been observed in patients with HPS-1, HPS-2, and HPS-4, but not HPS-3 or Chediak-Higashi syndrome (CHS), a disorder with features that overlap with HPS (4, 5). We aimed to determine whether susceptibility to bleomycin-induced fibrosis in HPS mouse models was limited to HPS mutations associated with lung fibrosis in humans with these different albinism syndromes. Bleomycin-induced 14-day mortality was 90 to 100% in HPS1*mt*, HPS2*mt,* and HPS2*ko* mice, all genotypes associated with human fibrosis. In marked contrast, mortality was 0 to 10% in bleomycin-challenged wild-type, HPS3*mt*, and CHS*mt* mice (Figure 1a), genotypes not known to be associated with human fibrosis. Lung histology and total collagen content were normal in unchallenged HPS and CHS mice up to 12 weeks of age (not shown). However, 7 days after bleomycin challenge, histologic evidence of diffuse fibrosis with substantial architectural distortion was evident in HPS1*mt*, HPS2*mt*, and HPS2*ko* mice (Figure 1b; Figure E1 in the online supplement). Only limited injury and pulmonary fibrosis was observed in bleomycin-challenged HPS3*mt* and CHS*mt* mice. Consistent with these results, total lung collagen content at Day 7 was not significantly different in bleomycin-challenged HPS3*mt* or CHS*mt* mice in comparison with wild-type mice, but was significantly elevated in bleomycin-challenged HPS1*mt*,

TABLE 1. MOUSE MODELS AND HUMAN DISEASE CORRELATES

Mouse Model Abbreviation	Murine Strain and Mutation	Human Disease Correlate	Human: Pulmonary Phenotype	Human Disease: Other Clinical Features	Protein	Rationale for Study
Wild-type (WT)	C57BL/6J	n/a	n/a	n/a	n/a	Wild-type control
WT(GFP)	C57BL/6J ubiquitously expressing GFP (ubiquitin C promoter)	n/a	n/a	n/a	GFP+	Wild-type control for bone marrow transplant experiments
HPS1*mt*	*HPS1* mutations; Naturally occurring ("pale ear" mouse)	HPS-1	Pulmonary fibrosis	Albinism, bleeding, colitis	Novel, BLOC3	Correlate for HPS human genotype most commonly associated with fibrosis
HPS2*mt*	*HPS2* mutations: Naturally occurring inversion-duplication in *AP3b1* ("pearl" mouse)	HPS-2	Pulmonary fibrosis	Albinism, bleeding, neutropenia	Adaptor protein AP-3	Correlate for HPS human genotype associated with pulmonary fibrosis; AP-3 most amenable to study
HPS2*ko*	Targeted knock-out of *HPS2* (34)	HPS-2	Pulmonary fibrosis	Albinism, bleeding, neutropenia, HLH	Adaptor protein AP-3	Comparison with HPS2*mt,* particularly with transgenic correction
HPS3*mt*	*HPS3* mutations; Naturally occurring ("cocoa" mouse)	HPS-3	No pulmonary fibrosis	Albinism, bleeding, colitis	Novel, BLOC2	Correlate for HPS human disease not associated with fibrosis
CHS*mt*	*Lyst/J* mutations Naturally occurring ("beige" mouse)	CHS	No pulmonary fibrosis	Recurrent infections	Lyst	Other disease control, not associated with fibrosis
HPS2:TG$^+$	HPS2*mt* or HPS2*ko* with transgenic correction of AP3b1 in the lung epithelium	n/a	n/a	n/a	Adaptor protein AP-3	Transgenic model developed

Definition of abbreviations: AP-3 = adaptor protein 3; BLOC = biogenesis of lysosomal organelle complex; CHS = Chediak-Higashi syndrome; GFP = green fluorescent protein; HLH = hemophagocytic lymphohistiocytosis; HPS = Hermansky-Pudlak syndrome; *ko* = knock-out; *mt* = mutant; n/a = not applicable.

HPS2*mt*, and HPS2*ko* mice (Figure 1c). Collectively, these results demonstrate that HPS mouse models faithfully replicate the fibrotic susceptibility of human HPS genotypes.

Genotype of Bone Marrow–derived Cells Does Not Determine Fibrotic Susceptibility

Alveolar macrophage dysregulation has been reported in patients with HPS-1 before the onset of pulmonary fibrosis (19). To determine whether macrophage dysfunction contributes to the disease pathogenesis, we generated reciprocal bone marrow chimeric mice. Fluorescence-activated cell sorter analysis of spleen cell populations revealed that donor cells accounted for 99.1 ± 0.9% of cells in HPS2*mt* recipients of wild-type marrow and 99.0 ± 0.8% of cells in wild-type recipients of HPS2*mt* marrow 90 days after transplantation (Figures 2a and 2b). In whole lung leukocyte populations, donor cell percentages were 95.2 ± 2.7% and 97.8 ± 1.4% for HPS2*mt* and wild-type recipients, respectively (Figures 2c and 2d). Greater than 93% of bronchoalveolar lavage (BAL) leukocytes were of donor origin in all transplanted mice (Figure 2e).

At more than 90 days after bone marrow transplantation, survival, lung histology, and collagen content in unchallenged mice were unchanged compared with age-matched control mice (not shown). After bleomycin exposure, excess mortality occurred in HPS2*mt* recipients despite transplantation with wild-type marrow (Figure 3a). Conversely, no mortality occurred, and lung histology revealed little evidence of fibrosis in wild-type mice that received HPS2*mt* marrow. Despite transplantation with wild-type marrow, HPS2*mt* mice displayed diffuse histologic evidence of pulmonary fibrosis and increased lung collagen content after bleomycin challenge without improvement compared with HPS2*mt* chimeric control mice (Figures 3b and 3d, Figure E2). To exclude potentially confounding influences from the small number of remaining host macrophages that are known to persist at earlier time points (36), we also studied a cohort of mice at 220 days after marrow transplantation. In this study, total lung collagen content at 7 days after bleomycin was 244 ± 13.5 μg for HPS2*mt* recipients of wild-type marrow and 236.1 ± 27.2 μg for HPS2*mt* recipients of HPS2*mt* marrow (not significant). To further confirm the relevance of these findings to HPS-1 disease, we also performed selected bone marrow transplantation experiments with HPS1*mt* mice. We found that transplantation of wild-type marrow failed to rescue the fibrotic susceptibility of recipient HPS1*mt* mice. Furthermore, transplantation of HPS1*mt* marrow into wild-type mice did not confer fibrotic susceptibility (Figures 3c and 3d). These data indicate that fibrotic susceptibility derives from genetic defects in nonhematopoietic cells.

The Alveolar Macrophage Activation Phenotype in HPS Mice Is Not Corrected by Bone Marrow Transplantation

Our prior studies have demonstrated that HPS1*mt* and HPS2*mt* murine alveolar macrophages exhibit enhanced basal production of cytokines, chemokines, and nitric oxide as well as hyperresponsiveness to LPS and other toll-like receptor agonists (20). We have also shown that BAL fluid from HPS mice has macrophage-activating capability for wild-type alveolar macrophages. Here, we used bone marrow chimeric mice to determine whether macrophage dysfunction is intrinsic to HPS mononuclear cells. Alveolar macrophages were isolated from unchallenged mice 90 days after bone marrow transplantation. The genotype of the recipient, but not the bone marrow donor, determined the macrophage activation phenotype as assessed by basal levels of tumor necrosis factor (TNF)-α and macrophage inflammatory protein (MIP)-1α in the cell culture media supernatant (Figures 3e–3h). Our studies indicate that the HPS activated macrophage phenotype does not appear to derive from a cell-autonomous defect.

Generation of hSPC-AP3b1 Transgenic Mice

Although most pulmonary fibrosis occurs in patients with HPS-1, ILD also occurs in patients with HPS-2 (4, 6), and the body of biochemical information and reagents available to study HPS-2

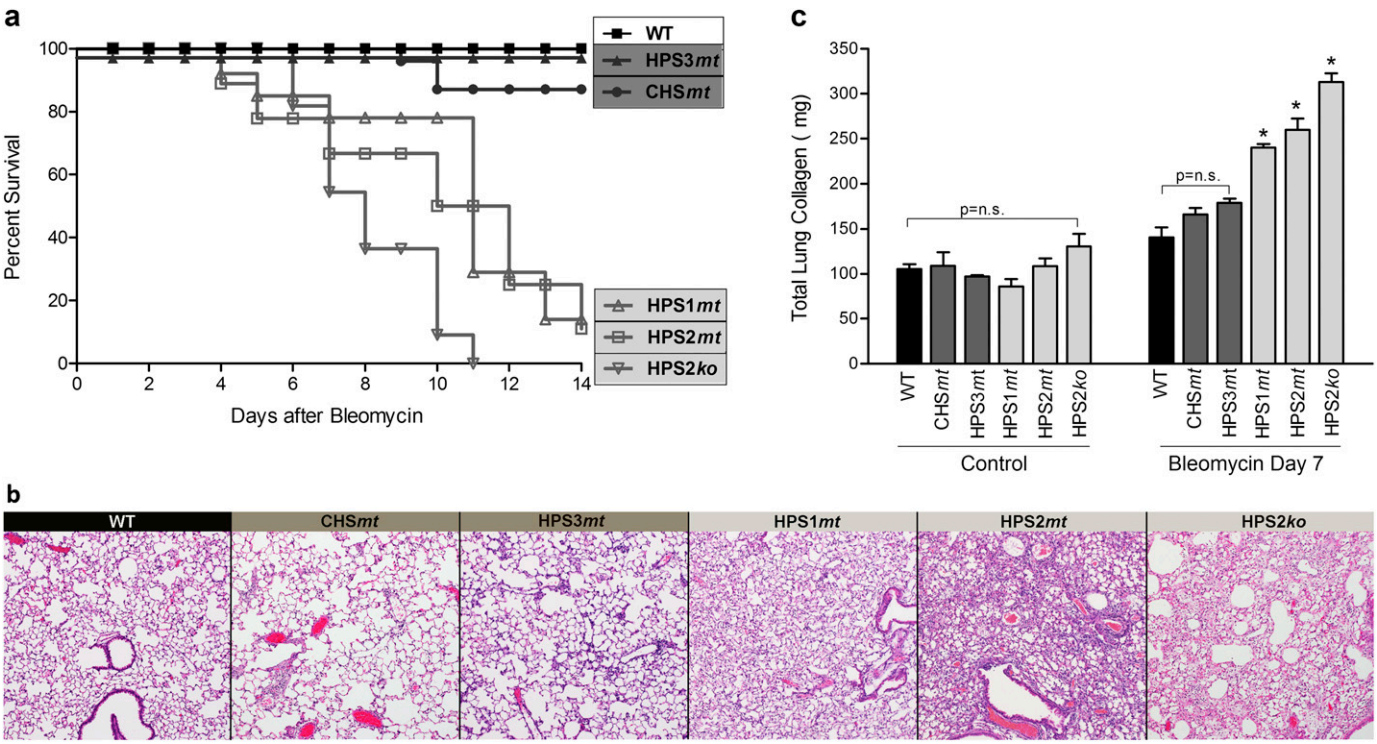

Figure 1. Susceptibility to bleomycin-induced pulmonary fibrosis occurs only in those Hermansky-Pudlak syndrome (HPS) mouse models corresponding to genotypes linked to human lung fibrosis. HPS1*mt*, HPS2*mt*, HPS2*ko*, HPS3*mt*, CHS*mt*, and strain-matched C57BL/6J wild-type (WT) mice, aged 8 to 12 weeks, were challenged by intratracheal instillation of a single bleomycin dose of 0.025 units. (*a*) Survival of HPS1*mt*, HPS2*mt*, and HPS2*ko* mice was significantly different from WT, HPS3*mt*, and CHS*mt* when analyzed by log-rank test (n = 8 per group minimum; $P < 0.01$ for HPS1*mt*, HPS2*mt*, and HPS2*ko* versus other groups, with adjustment for multiple comparisons). (*b*) Representative lung histology images (hematoxylin and eosin, 10× magnification) obtained 7 days after mice were challenged with bleomycin. *Light gray labels* denote models corresponding to HPS genotypes associated with pulmonary fibrosis (HPS-1 and HPS-2) and *dark gray labels* denote models corresponding to human genotypes that have not been associated with pulmonary fibrosis (HPS-3 and Chediak-Higashi syndrome [CHS]). (*c*) Collagen quantitation using the Sircol Red assay from lungs harvested 7 days after bleomycin or controls. Values indicate totals for both lungs from each mouse; n = 12 per group for WT and HPS2*mt*, n = 8 per group for others. *$P < 0.001$ versus WT bleomycin challenged (analysis of variance with Tukey post-test).

are more robust (26, 33, 34, 37, 38). To directly test whether fibrotic susceptibility of HPS2*mt* mice originates from the pulmonary epithelium, we developed a transgenic model with epithelial-specific correction of the β3a subunit of AP-3 in the lungs of HPS2*mt* mice (Figures 4a–4c). Mutations in individual AP-3 subunits (such as β3 in HPS2*mt* mice) are known to result in instability and ubiquitin-mediated degradation of the entire AP-3 complex. Therefore, loss and functional restoration of the β3A protein product can be documented by the absence or presence, respectively, of other AP-3 subunits (26). Transgene $(TG)^+$ mice, but not TG^{neg} mice, showed functional correction of AP-3 stability in type II epithelial cells and lung but not the spleen, as revealed by the presence of the μ3 subunit or the delta subunit (Figures 4d and 4e). Faint bands detected in TG^{neg} HPS2*mt* mice are consistent with prior reports that the HPS2*mt* is a hypomorph (34). We confirmed our findings in a second founder line and found no difference in the extent of functional correction and rescue. We found that HPS1*mt* (not shown) and HPS2*mt* type II cells secreted levels of monocyte chemotactic protein (MCP)-1 that were more than threefold greater than wild-type type II cells and that epithelial transgenic *AP3b1* expression in HPS2*mt* mice significantly corrected the exaggerated MCP-1 secretion (Figure 4f). A similar pattern was observed for type II cell secretion of chemokine (C-X-C motif) ligand 1 (CXCL1) (Figure 4g). Type II cells in patients and mice with HPS have been reported to contain enlarged lamellar bodies. Epithelial correction of AP3b1 also resulted in significant reduction in lamellar body size in HPS2*mt* mice (Figure 4h, Figure E3).

Epithelial-Specific Correction of AP3b1 Protects HPS2*mt* Mice from Bleomycin-induced Mortality and Pulmonary Fibrosis

In comparison with HPS2*mt* TG^{neg} littermate control mice, 6- to 8-week-old HPS2*mt* TG^+ mice had significantly reduced mortality after bleomycin challenge (Figure 5a). Seven days after bleomycin was administered, mortality was greater than 50% in TG^{neg} mice, whereas all TG^+ mice were alive at this time point, although mortality subsequently occurred with a delayed time course. Lung histology and collagen content were analyzed 7 days after bleomycin challenge in surviving mice. Histologic evidence of fibrosis was present in TG^+ mice but was mild in degree compared with the surviving TG^{neg} mice (Figure 5b and Figure E4). Both founder lines of TG^+ HPS2*mt* mice had significant reduction in total lung collagen content compared with their TG^{neg} littermate control mice, although levels remained greater than those of wild-type mice (Figure 5c). One founder line was also back-crossed into HPS2*ko* mice to determine whether the mutant HPS2 allele interfered with transgene expression. A similar reduction in the extent of bleomycin-induced lung collagen accumulation was observed when the high expression founder line was back-crossed into HPS2*ko* mice (Figure 5c). Interestingly, epithelial-specific correction of AP-3 in HPS2*mt* mice also resulted in significant reduction in alveolar macrophage production of TNF-α and

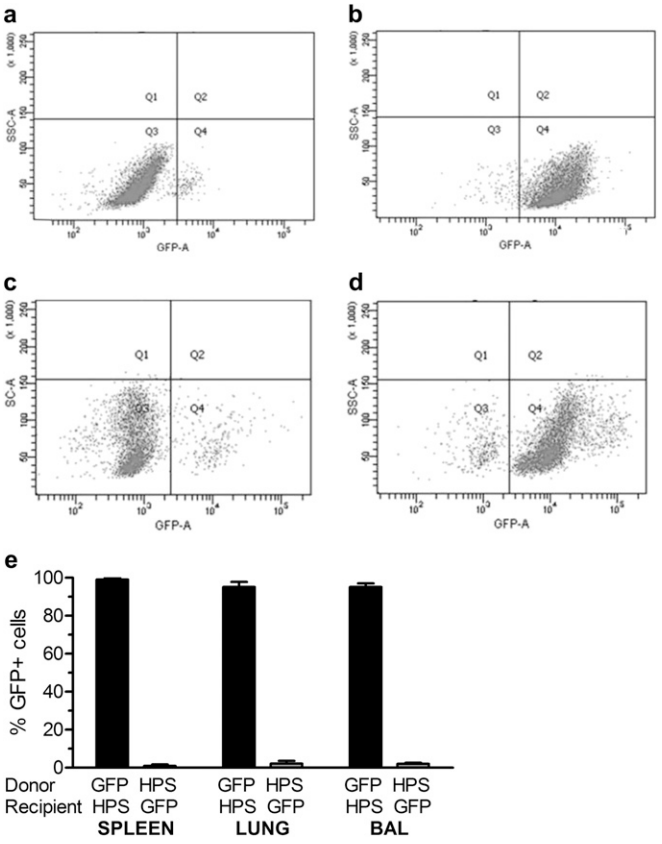

Figure 2. Generation of bone marrow chimeras. (*a*, *b*) Representative fluorescence-activated cell sorter (FACS) analysis of spleen cell populations 90 days after bone marrow transplantation. C57BL/6J mice that express green fluorescent protein (GFP) under the control of the ubiquitin promoter were used as wild-type (WT) mice in these experiments. (*a*) Results from a WT(GFP) recipient of HPS2*mt* marrow. (*b*) HPS2*mt* recipient of WT(GFP) marrow. (*c*, *d*) Representative FACS analysis of lung leukocyte populations 90 days after bone marrow transplantation. (*c*) Results from a WT(GFP) recipient of HPS2*mt* marrow. (*d*) HPS2*mt* recipient of WT(GFP) marrow. (*e*) Quantitation of the percentage of donor cell reconstitution in the spleen, whole lung, and bronchoalveolar lavage (BAL) 90 days after bone marrow transplantation. Results of FACS analysis and BAL cytospins were quantitated from three mice in each transplantation group.

MIP-1α compared with TG^{neg} littermate control mice (Figures 5d and 5e). Taken together with the failure of bone marrow transplantation to rescue the macrophage phenotype, these data indicate that HPS mutations in alveolar epithelial cells are responsible for alveolar macrophage activation.

Extent of Alveolar Type II Cell Apoptosis Is Dependent on HPS Genotype and Is a Key Early Event Determining Fibrotic Susceptibility in HPS Mice

Consistent with our previous findings that the early inflammatory response is similar in wild-type and HPS2*mt* mice (18), we also found no differences in indicators of lung injury after bleomycin challenge, including wet-to-dry lung weight ratios and BAL protein levels (Figure E5). However, 5 hours after bleomycin challenge, HPS1*mt*, HPS2*mt*, and the HPS2*ko* mice had prominent and accelerated type II cell apoptosis (Figure 6a), in contrast to the minimal numbers of TUNEL-positive type II cells in wild-type, HPS3*mt*, and CHS*mt* mice. Furthermore, we found that expression of *AP3b1* in HPS2*mt* type II cells reduced the extent of type II cell apoptosis compared with HPS2*mt*-TG^{neg} mice (Figure 6b and Figure E6). *In vitro* studies with isolated type II cells from unchallenged HPS2*mt* mice confirmed a dose-dependent susceptibility to bleomycin-induced cell death that was greater than that of wild-type cells (Figure 6c).

We tested the effect of prophylactic pan-caspase inhibition to determine whether apoptosis played a causal role in the fibrotic susceptibility of HPS mice. Starting 24 hours before intratracheal bleomycin challenge, HPS2*mt* or wild-type mice received quinolyl-valyl-O-methylaspartyl-[-2,6-difluorophenoxy]-methyl ketone (Q-VD-Oph, intraperitoneal dosing 20 mg/kg, every other day) or vehicle (dimethyl sulfoxide) control. At 7 days after bleomycin challenge, mortality was 0% in wild-type mice, 10% in the HPS2*mt* group treated with Q-VD-Oph, and 30% in the vehicle (dimethyl sulfoxide)-treated HPS2*mt* group. Bleomycin-challenged HPS2*mt* mice treated with the pan-caspase inhibitor exhibited lung collagen content at 7 days that was no greater than that observed in wild-type mice (Figure 6d). Collectively, these data suggest that AP-3 deficiency is responsible for enhanced type II cell apoptosis in HPS2*mt* mice and that epithelial apoptosis plays a mechanistic role in the fibrotic susceptibility of HPS mice.

Mahavadi and colleagues have previously reported that ER stress underlies epithelial apoptosis in HPS, based in part on studies performed in HPS1/2 double-mutant mice at an advanced age when fibrosis was present (23). To determine whether ER stress could underlie the increased susceptibility to epithelial cell apoptosis in our models, we performed comprehensive ER stress–associated gene and protein expression studies in type II cells and whole lung tissue from HPS1*mt* and HPS2*mt* mice. We found no evidence of increased ER stress in HPS mutants compared with wild-type control mice at baseline or after bleomycin challenge that could explain the observed early epithelial apoptosis (Figures E7–E10).

DISCUSSION

Through murine bone marrow transplantation and generation of a transgenic model with epithelial-specific gene correction, our studies demonstrate that the pulmonary epithelium is paramount in the fibrotic susceptibility of HPS mice. Targeted reexpression of the missing subunit of the AP-3 complex in the lung epithelium of HPS2*mt* mice restored type II cell homeostasis, including cytokine production and lamellar body size, and reduced subsequent susceptibility to bleomycin-induced early type II cell apoptosis and fibrosis. In contrast, bone marrow transplantation did not protect HPS recipients from excess bleomycin-induced fibrosis. Similarly, dysregulated alveolar macrophage activation was determined by the recipient and not the donor, and transgenic correction in alveolar epithelial cells reduced cytokine production by alveolar macrophages, suggesting that the activated macrophage phenotype seen in HPS is regulated through a paracrine mechanism. Together, our data indicate that intracellular trafficking defects secondary to HPS mutations in alveolar epithelial cells contribute to the profibrotic phenotype in HPS through increased vulnerability to apoptosis and a persistent state of epithelial-driven macrophage activation in the lungs.

We studied a number of different mouse models corresponding to HPS genotypes that are either associated or not associated with human pulmonary fibrosis. As an additional disease control, we studied Chediak-Higashi syndrome mice, a related trafficking disorder with overlapping clinical features and giant lamellar bodies in type II cells but no reported pulmonary fibrosis in patients. Bleomycin is a chemotherapeutic agent associated with pulmonary inflammation, interstitial expansion, and irreversible pulmonary fibrosis in humans. Although widely studied, the

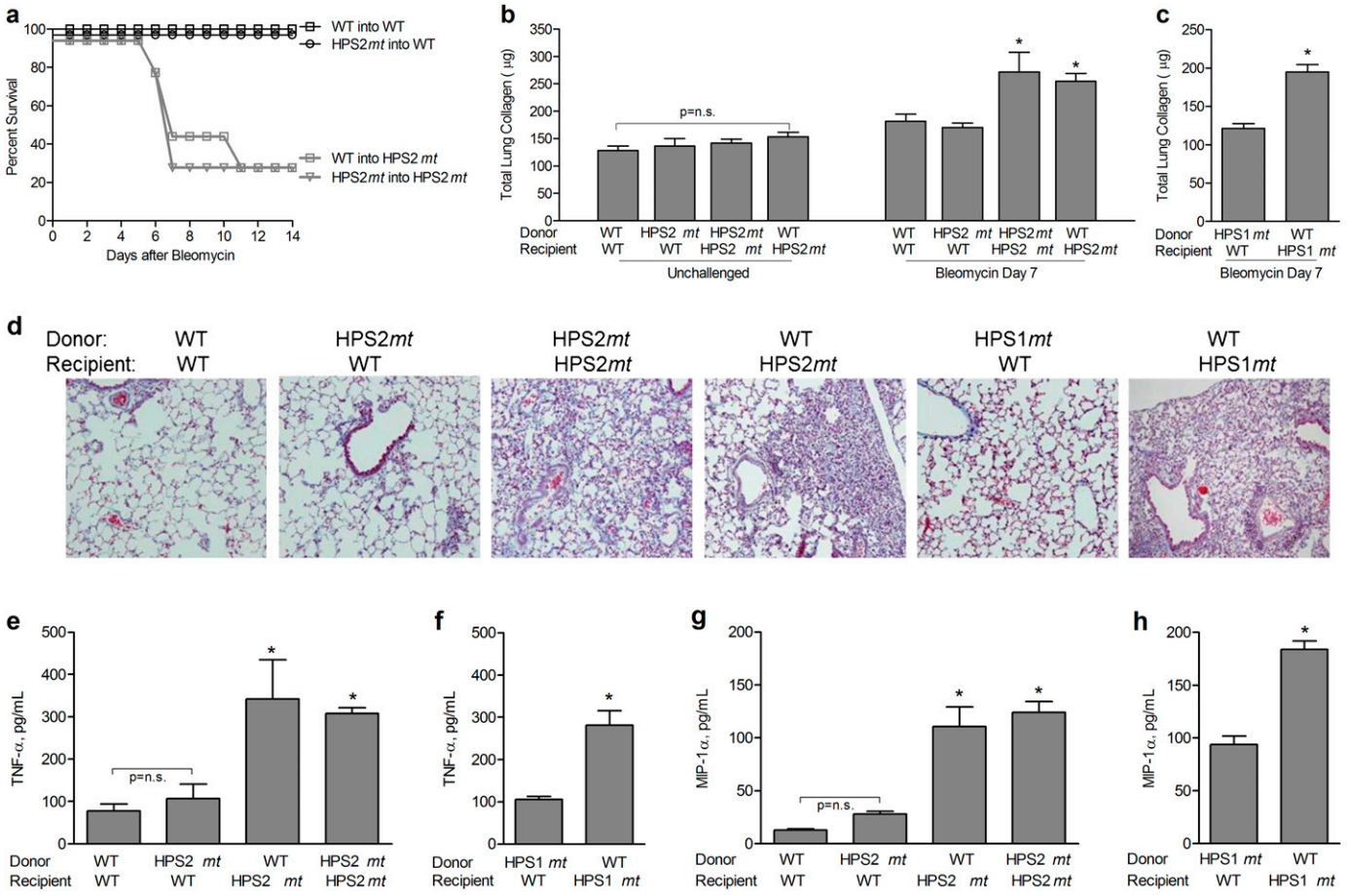

Figure 3. Bone marrow transplantation of wild-type (WT) whole marrow fails to rescue the fibrotic susceptibility of HPS2*mt* and HPS1*mt* mice, and transplantation of HPS2*mt* or HPS1*mt* marrow into WT mice does not confer fibrotic susceptibility. Transplanted mice, age 20 to 26 weeks, were studied 90 days after bone marrow transplantation. Mice were challenged with a single intratracheal dose of bleomycin, 0.025 units. (*a*) Survival of bone marrow–transplanted HPS2*mt* and WT mice after bleomycin challenge. HPS2*mt* mice (*gray*) show increased mortality after bleomycin challenge despite transplantation with WT marrow. WT mice (*black*) had no mortality after bleomycin challenge despite transplantation with HPS2*mt* marrow. Chimeric mice (WT into WT and HPS2*mt* into HPS2*mt*) were used as experimental control groups. n = 6–10 per group; $P <$ 0.001 for HPS2*mt* versus WT recipients by log-rank test. (*b*) Quantitation of lung collagen content demonstrates that increased pulmonary fibrosis occurs in the bleomycin-challenged HPS2*mt* mice despite transplantation with WT marrow. Lungs were harvested 7 days after bleomycin challenge and assayed using the Sircol Red assay. Values indicate totals for both lungs from each mouse; n = 3 per group for unchallenged, n = 10 for HPS2*mt* recipients of WT marrow, and n = 5 for other combinations. $P =$ not significant among unchallenged mice at baseline, $*P < 0.001$ versus WT recipients after bleomycin challenge (analysis of variance with Tukey post-test). (*c*) Quantitation of lung collagen content in HPS1*mt* bone marrow transplant experiments. Mice were challenged with bleomycin 90 days after marrow transplantation, and lung collagen was evaluated 7 days later. n = 7 for HPS1*mt* recipients of WT marrow and n = 5 for WT recipients of HPS1*mt* marrow, $*P < 0.01$. (*d*) Representative lung histology images with Trichrome staining (20× magnification), 7 days after bleomycin challenge, are shown from each of the transplanted groups. Note that only minimal fibrosis is present in WT recipients, even after transplantation with HPS2*mt* or HPS1*mt* marrow. In contrast, severe fibrosis occurs in HPS2*mt* and HPS1*mt* recipients, despite transplantation of WT marrow. (*e–h*) Impact of bone marrow transplantation on alveolar macrophage activation phenotype of constitutive cytokine secretion. Alveolar macrophages were isolated by bronchoalveolar lavage and cultured, and tumor necrosis factor (TNF)-α (*e*, *f*) and macrophage inflammatory protein (MIP)-1α (*g*, *h*) were assayed from the cell culture media supernatant by ELISA. For *e* and *g*, n = 4–8 per group, $*P < 0.05$ for both HPS2*mt* recipients versus WT recipients. For *f* and *h*, n = 6 for WT recipients of HPS1*mt* marrow, n = 10 for HPS1*mt* recipients of WT marrow, $*P < 0.05$.

bleomycin mouse model recapitulates only the first two of these features, and its value as a mimic of human disease is debated (39). Our findings that the fibrotic susceptibility of HPS mice to bleomycin segregates with HPS genotypes associated with pulmonary fibrosis in humans support the validity of the bleomycin model as a read-out of HPS fibrotic susceptibility.

Alveolar macrophage dysfunction has been implicated in the pulmonary fibrosis that occurs in patients with HPS (19), and our previous studies have demonstrated that HPS mice have constitutive alveolar macrophage activation that mimics the human phenotype (20). Therefore, we performed comprehensive whole marrow transplantation studies in HPS2*mt* and HPS1*mt* mice. As controls, HPS2*mt* mice were transplanted with HPS2*mt* marrow, to exclude potential confounding effects of irradiation. Furthermore, we studied mice at conservatively late time points after transplant to limit any potential contribution from the small numbers of resident host macrophages that are known to persist after transplant (36). We found that transplantation of wild-type marrow failed to rescue the fibrotic susceptibility of HPS1*mt* and HPS2*mt* recipient mice. Although bone marrow transplantation has been proposed for HPS, extrapolation of our findings would suggest that bone marrow transplantation is unlikely to protect

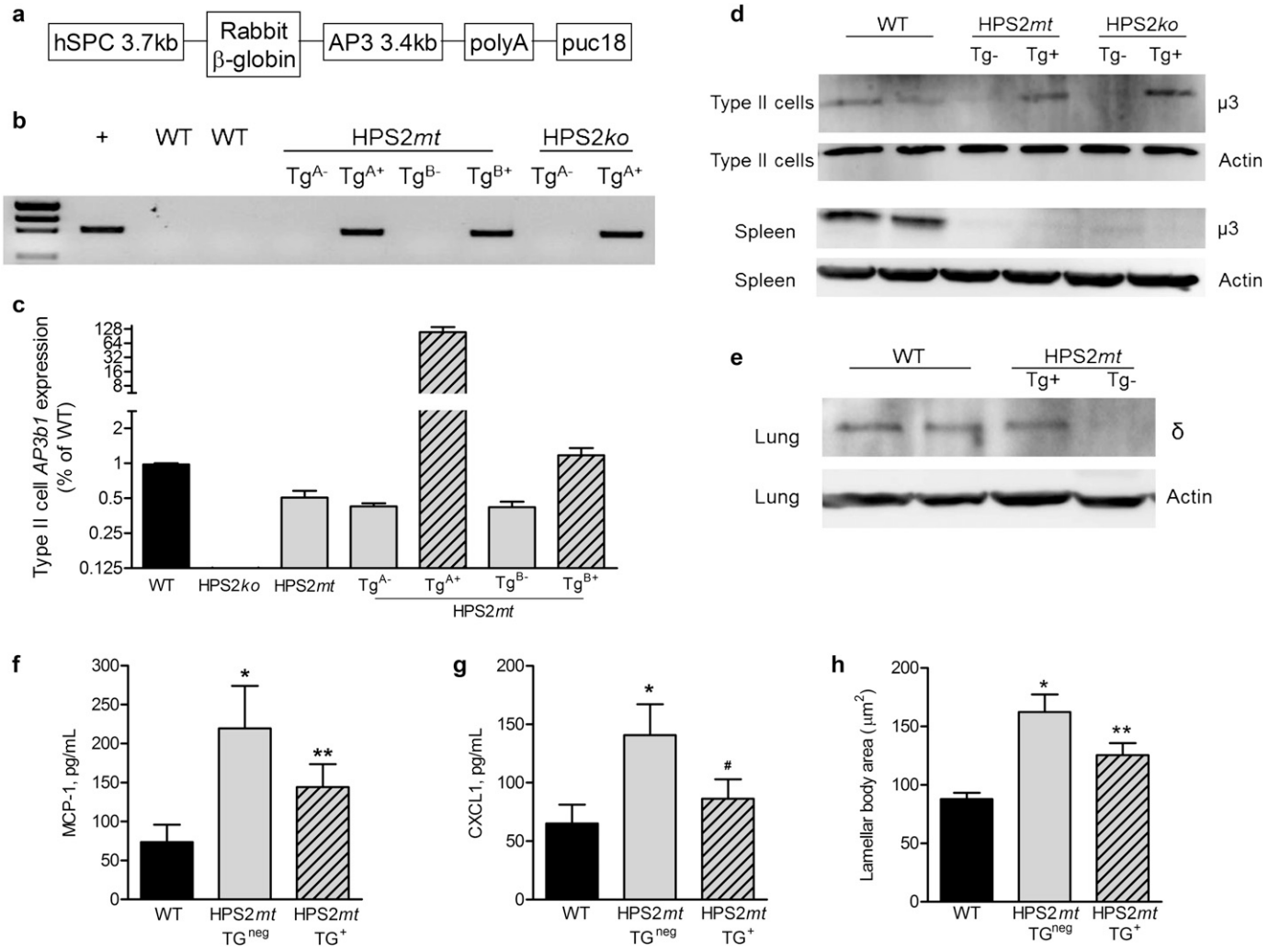

Figure 4. Transgenic correction of the defective β3 subunit stabilizes the AP-3 complex as evidenced by detection of the mu and delta subunits of the heterooligomer. (*a*) Construct used for generation of hSPC-AP3 transgenic mice. The cDNA for murine AP-3/β3A was generated by polymerase chain reaction (PCR) amplification, fully sequenced, and inserted into a vector containing the human SP-C promoter and β-globin sequences as follows: hSPC promoter (3.7 kb)–intronic β globin sequence–AP3 (3.4 kb)–β globin–poly A. This construct was linearized and injected into the pronuclei of fertilized mouse C57BL/6J embryos and implanted into pseudopregnant C57BL/6J dams. Progeny were screened by PCR to identify founders, which were then crossed back into HPS2*mt* or HPS2*ko* mice. (*b*) PCR detection of a sequence spanning the hSPC promoter to rabbit β-globin. HPS2*mt* and HPS2*ko* denote the background HPS2 mice, and (+) represents the plasmid for the positive control. The PCR strategy distinguishes transgene-positive mice from two different founder lines (TG^{A+} and TG^{B+}) from wild-type (WT) and transgene-negative mice (TG^{A-} and TG^{B-}). (*c*) Quantitative PCR analysis of AP3b1 from alveolar type II cells from transgene-positive, transgene-negative, and WT mice. Data were normalized to Actb. Note that AP3b1 was not detected from HPS2*ko* mice. $^{*}P < 0.05$ versus WT, $^{\#}P < 0.05$ versus HPS2*mt*, HPS2*ko*, TG^{A-} and TG^{B-}, and P = not significant, versus WT, $^{**}P < 0.01$ versus all others. (*d*) Rescue of the AP-3 complex stability as demonstrated by presence of μ3 in transgene-positive mice. Western blots of cells isolated from HPS2*mt* mice show stabilization of the AP-3 μ3 subunit in alveolar type II cells in transgene-positive mice (TG^{+}), but not in the spleen, nor in transgene-negative (TG^{neg}) mice. β-actin expression is shown as the loading control. (*e*) Rescue of the AP-3 complex as demonstrated by delta (δ) subunit detection in transgene-positive mice. Example Western blot using a monoclonal antibody to the delta subunit confirms functional expression of the β3 subunit in transgene-positive (TG^{+}) mice. The delta subunit is not detected in the HPS2*mt* TG^{neg} mice. β-actin expression is shown as the loading control. (*f*, *g*) Epithelial-specific transgenic correction of AP-3 reduces excess monocyte chemotactic protein (MCP)-1 and chemokine (C-X-C motif) ligand 1 (CXCL1) production from HPS2*mt* alveolar type II cells. MCP-1 and CXCL1 levels were assayed from conditioned media of unchallenged primary murine alveolar type II cells. For *f*, $^{*}P < 0.01$ versus WT and TG^{+}, $^{**}P < 0.05$ versus WT. For *g*, $^{*}P < 0.01$ versus WT and $^{\#}P < 0.05$ versus WT and TG^{neg}, n = 9 to 12 per group. (*h*) Epithelial-specific transgenic correction of AP-3 also reduces the size of enlarged lamellar bodies in HPS2*mt* alveolar type II cells. Images of lamellar bodies were captured by a technician blinded to the genotype of samples, and the area of lamellar bodies was quantitated on 10,000× images of the ultrastructural examination using Olympus Soft Imaging Solutions. $^{*}P < 0.01$ versus WT and $^{**}P < 0.05$ versus WT and TG^{neg}.

patients with HPS from pulmonary fibrosis. Furthermore, because the bleeding complications of HPS generally respond favorably to routine platelet transfusion, bone marrow transplantation is not usually considered for the sole purpose of reducing bleeding risk. Several murine studies demonstrate that the lung recruits circulating bone marrow–derived cells to aid in repair after bleomycin-induced injury (40–43). Our data demonstrate that HPS defects in bone marrow–derived cells are not sufficient for fibrotic susceptibility in HPS mice. However, we have not excluded the possibility that bone marrow–derived cells play a secondary role as effector cells in promoting or mitigating HPS pulmonary fibrosis.

Given the results of the bone marrow transplant experiments, we proceeded to directly test the role of HPS mutations in the

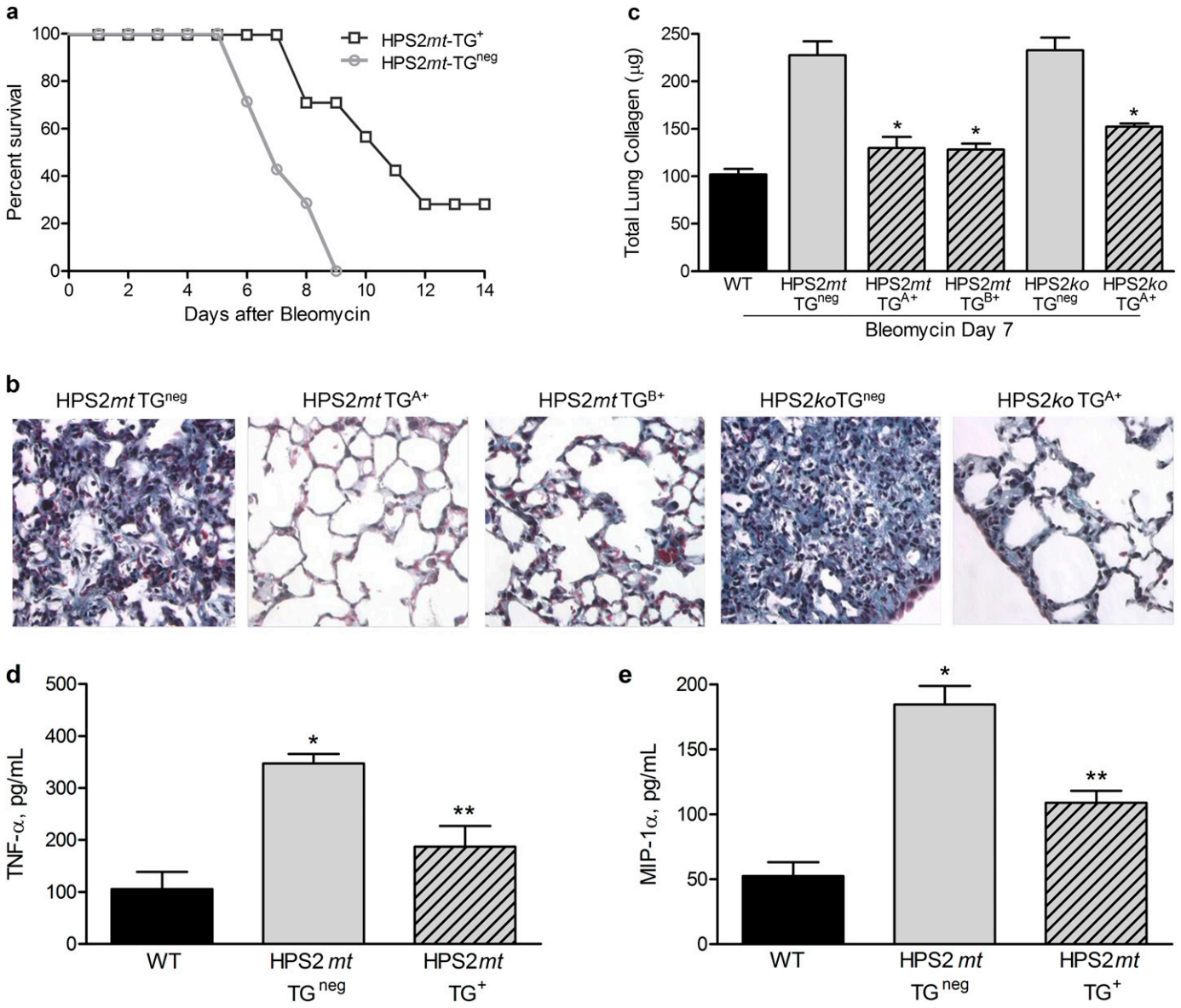

Figure 5. Epithelial-specific transgenic correction of AP-3 protects Hermansky-Pudlak syndrome (HPS) mice from bleomycin-induced mortality and pulmonary fibrosis and also dampens constitutive alveolar macrophage activation. (*a*) Increased survival of transgene-positive HPS mice after intratracheal bleomycin challenge. Transgene-positive (*open squares*) and transgene-negative (*circles*) HPS2*mt* mice, aged 6 to 8 weeks, were challenged by intratracheal instillation of a single bleomycin dose of 0.025 units per mouse. Survival was significantly increased in the transgene-positive HPS2*mt* mice based on analysis using the log-rank test (n = 7 per group, $P < 0.01$). (*b*) Trichrome staining (40×) of representative lung histology images from Day 7 bleomycin-challenged transgene-positive mice and littermate control mice, for HPS2 transgene-negative (HPS2 TG^{neg}), both HPS transgene-positive lines (HPS2*mt*-TG^{A+} and HPS2*mt*-TG^{B+}), and HPS2*ko* transgene-positive and -negative mice. (*c*) Quantitation of the total lung collagen content demonstrates that the transgene-positive HPS2*mt* and HPS2*ko* mice are relatively resistant to bleomycin-induced fibrosis compared with transgene-negative littermate control mice. Mice were challenged with intratracheal bleomycin, and lungs were harvested for Sircol collagen assay on Day 7. n = 6 each for all groups except n = 9 each for HPS2*mt* TG^{A+} and TG^{neg}. *$P < 0.01$ versus TG^{neg} mice and $P < 0.05$ versus wild-type mice. (*d, e*) Epithelial-specific transgenic correction of AP-3 also corrects the alveolar macrophage activation phenotype. Primary alveolar macrophages were isolated by bronchoalveolar lavage and cultured, and tumor necrosis factor (TNF)-α (*d*) and macrophage inflammatory protein (MIP)-1α (*e*) were assayed in the alveolar macrophage cell culture media supernatant by ELISA. *$P < 0.01$ versus WT and TG^{neg}, **$P < 0.05$ versus WT, n = 6 to 12 per group.

lung epithelium of mice. In our transgenic model, epithelial-specific correction resulted in highly significant, but incomplete, protection from bleomycin injury compared with littermate control mice. The direction and degree of phenotypic correction was consistent across all outcome parameters studied, including histology, collagen content, cytokine production, apoptosis, and mortality. There was no difference in the extent of protection in a high versus lower expressing transgenic line. There are a number of known limitations of this transgenic model system that may explain incomplete correction of the pulmonary phenotype in HPS mice, including that expression driven with the human SP-C promoter is known to be variable and restricted to a subset of lung epithelial cells (44, 45). Furthermore, allergic inflammation has been reported to down-regulate SP-C promoter expression (46), and bleomycin may cause time-dependent attenuation of *AP3b1* transgenic expression. Finally, we find that dominant negative interference

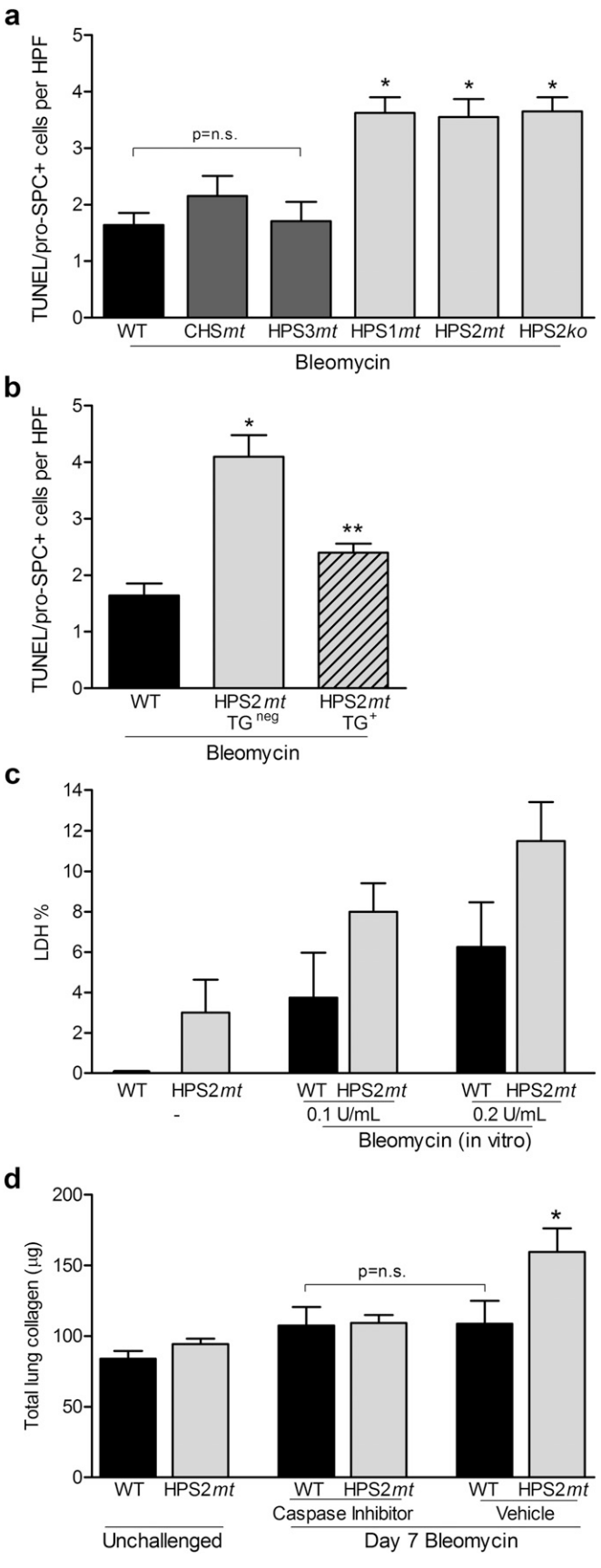

Figure 6. Alveolar epithelial apoptosis correlates with fibrotic susceptibility in Hermansky-Pudlak syndrome (HPS) mice. (*a*) Evaluation of early alveolar apoptosis in HPS mouse models. Lungs were inflation-fixed 5 hours after intratracheal bleomycin challenge, terminal deoxynucleotidyl transferase-mediated dUTP nick end labeling (TUNEL) assay, and pro-SP-C immunofluorescence were performed, and the mean number of dual-positive cells (TUNEL-positive, pro-SP-C positive type II cells) were determined from a minimum of 10 fields counted by two independent observers blind to mouse genotype. n = 3–6 per group, P = not significant (n.s.) for unchallenged mice (not shown). P = n.s. for wild-type (WT) versus CHS*mt* and HPS3*mt* 5 hours after bleomycin, and $*P < 0.01$ for HPS1*mt*, HPS2*mt*, and HPS2*ko* versus WT, CHS*mt*, or HPS3*mt* (analysis of variance [ANOVA]). (*b*) Quantitation of TUNEL-positive type II cells from WT, HPS2*mt*-TG^{neg}, and HPS2*mt*-TG^{+} mice. n = 4 mice per group, $*P < 0.001$ for TG^{neg} versus WT, $**P < 0.01$ for TG^{+} versus TG^{neg} littermate control mice, and P = n.s. for TG^{+} versus WT. (*c*) Bleomycin-induced cell death in primary murine type II cells *in vitro*, measured by lactate dehydrogenase (LDH) cytotoxicity assay. Primary murine type II cells were isolated and cultured *in vitro*, and LDH was expressed as LDH% (LDH media/LDH cells + media) compared with WT control. n = 4 mice per group; $P < 0.0001$ for both mouse strain and bleomycin dose effect by two-way ANOVA. (*d*) Pan-caspase inhibition protects HPS mice from excess bleomycin-induced pulmonary fibrosis. HPS*2mt* or WT mice, aged 8 to 10 weeks, were challenged with intratracheal bleomycin 24 hours after initiation of intraperitoneal caspase inhibitor Q-VD-Oph or vehicle control (dimethyl sulfoxide), and the total lung collagen content was measured by Sircol assay 7 days after the bleomycin challenge. n = 10 for WT and HPS2*mt* with caspase inhibitor, n = 10 for WT with vehicle, and n = 7 for HPS2*mt* with vehicle control. $*P < 0.01$ versus all other groups. P = n.s. for HPS2*mt* with caspase inhibitor versus all WT.

of endogenous mutant HPS proteins is unlikely, given that the extent of transgenic rescue observed was similar in the complete knock-out (HPS2*ko*) and the hypomorphic (HPS2*mt*) backgrounds. Our data do not exclude the possibility that additional mechanisms contribute to fibrotic susceptibility and mortality in HPS mice.

A striking and consistent abnormality in bleomycin-challenged HPS mice is the accelerated apoptosis of type II cells. The extent of alveolar epithelial apoptosis correlated with extent of fibrosis in different HPS mouse models, and transgenic epithelial correction of the *HPS2* defect resulted in significant reduction in type II cell apoptosis. Studies demonstrating that a pan-caspase inhibitor protected HPS mice from bleomycin-induced fibrosis provide additional evidence that apoptosis plays a causal role in HPS pulmonary fibrosis, although we cannot exclude effects the drug may have had on other cell types that could be playing a role in fibrosis. Although the albinism and bleeding phenotypes are fairly consistent across different HPS genotypes, pulmonary fibrosis is restricted to only certain HPS genotypes in humans, consistent with distinct and divergent trafficking functions of HPS proteins in the alveolar epithelium. The mechanistic relationship between HPS intracellular trafficking defects and epithelial vulnerability to apoptosis remain incompletely understood at this time. We propose that our data, in conjunction with experimental models using the Fas-Fas ligand system (14, 15) and transgenic diphtheria-toxin targeted ablation of the epithelium (16), support the concept that alveolar epithelial cell apoptosis is a key event in the pathogenesis of pulmonary fibrosis. However, although ER stress may be causal in some genetic forms of pulmonary fibrosis (47–49), alveolar epithelial vulnerability in HPS appears to occur by a different mechanism. As a result, further study of HPS trafficking defects may elucidate additional mechanisms responsible for pulmonary fibrosis.

In summary, our studies demonstrate that HPS fibrotic susceptibility is due to intracellular trafficking defects in the alveolar epithelium, which may also contribute to fibrosis through paracrine activation of alveolar macrophages. HPS mouse models

provide a tractable mimic of the human disease and will be valuable for further deciphering mechanisms of pulmonary fibrosis in HPS. Our hope is that insights gained from this rare genetic disease will have broader implications for understanding the pathogenesis of more common fibrotic lung diseases.

Author disclosures are available with the text of this article at www.atsjournals.org.

Acknowledgment: The authors thank Richard Swank for breeding pairs of HPS1*mt* pale ear and HPS2*mt* pearl mice, and Sally Mansour and Margit Burmeister for the AP3b1$^{-/-}$ mice (HPS2*ko*). We also thank Stephan Glasser and Jeffrey Whitsett for providing the human SP-C promoter, Andrew Peden for providing the original AP-3 delta subunit antibody, Jon Neumann in the Transgenic Mouse Core at the University of Cincinnati for technical assistance in the generation of the transgenic mice, and Jeff Bailey and Victoria Summey in The Comprehensive Mouse and Cancer Core at Cincinnati Children's Hospital Medical Center for technical assistance with murine bone marrow transplantation.

References

1. King TE Jr, Pardo A, Selman M. Idiopathic pulmonary fibrosis. *Lancet* 2011;378:1949–1961.
2. Gahl WA, Brantly M, Kaiser-Kupfer MI, Iwata F, Hazelwood S, Shotelersuk V, Duffy LF, Kuehl EM, Troendle J, Bernardini I. Genetic defects and clinical characteristics of patients with a form of oculocutaneous albinism (Hermansky-Pudlak syndrome). *N Engl J Med* 1998;338:1258–1264.
3. Cullinane AR, Curry JA, Carmona-Rivera C, Summers CG, Ciccone C, Cardillo ND, Dorward H, Hess RA, White JG, Adams D, *et al.* A BLOC-1 mutation screen reveals that PLDN is mutated in Hermansky-Pudlak syndrome type 9. *Am J Hum Genet* 2011;88:778–787.
4. Gochuico BR, Huizing M, Golas GA, Scher CD, Tsokos M, Denver SD, Frei-Jones MJ, Gahl WA. Interstitial lung disease and pulmonary fibrosis in Hermansky-Pudlak syndrome type 2, an adaptor protein-3 complex disease. *Mol Med* 2012;18:56–64.
5. Brantly M, Avila NA, Shotelersuk V, Lucero C, Huizing M, Gahl WA. Pulmonary function and high-resolution CT findings in patients with an inherited form of pulmonary fibrosis, Hermansky-Pudlak syndrome, due to mutations in HPS-1. *Chest* 2000;117:129–136.
6. Shotelersuk V, Dell'Angelica EC, Hartnell L, Bonifacino JS, Gahl WA. A new variant of Hermansky-Pudlak syndrome due to mutations in a gene responsible for vesicle formation. *Am J Med* 2000;108:423–427.
7. Pierson DM, Ionescu D, Qing G, Yonan AM, Parkinson K, Colby TC, Leslie K. Pulmonary fibrosis in Hermansky-Pudlak syndrome. A case report and review. *Respiration* 2006;73:382–395.
8. Gibbons MA, MacKinnon AC, Ramachandran P, Dhaliwal K, Duffin R, Phythian-Adams AT, van Rooijen N, Haslett C, Howie SE, Simpson AJ, *et al.* Ly6Chi monocytes direct alternatively activated profibrotic macrophage regulation of lung fibrosis. *Am J Respir Crit Care Med* 2011;184:569–581.
9. Sun L, Louie MC, Vannella KM, Wilke CA, LeVine AM, Moore BB, Shanley TP. New concepts of IL-10-induced lung fibrosis: fibrocyte recruitment and M2 activation in a CCL2/CCR2 axis. *Am J Physiol Lung Cell Mol Physiol* 2011;300:L341–L353.
10. Gangadharan B, Hoeve MA, Allen JE, Ebrahimi B, Rhind SM, Dutia BM, Nash AA. Murine gammaherpesvirus-induced fibrosis is associated with the development of alternatively activated macrophages. *J Leukoc Biol* 2008;84:50–58.
11. Murray LA, Rosada R, Moreira AP, Joshi A, Kramer MS, Hesson DP, Argentieri RL, Mathai S, Gulati M, Herzog EL, *et al.* Serum amyloid P therapeutically attenuates murine bleomycin-induced pulmonary fibrosis via its effects on macrophages. *PLoS ONE* 2010;5:e9683.
12. Prasse A, Pechkovsky DV, Toews GB, Jungraithmayr W, Kollert F, Goldmann T, Vollmer E, Muller-Quernheim J, Zissel G. A vicious circle of alveolar macrophages and fibroblasts perpetuates pulmonary fibrosis via CCL18. *Am J Respir Crit Care Med* 2006;173:781–792.
13. Tighe RM, Liang J, Liu N, Jung Y, Jiang D, Gunn MD, Noble PW. Recruited exudative macrophages selectively produce CXCL10 after noninfectious lung injury. *Am J Respir Cell Mol Biol* 2011;45:781–788.
14. Kuwano K, Hagimoto N, Kawasaki M, Yatomi T, Nakamura N, Nagata S, Suda T, Kunitake R, Maeyama T, Miyazaki H, *et al.* Essential roles of the Fas-Fas ligand pathway in the development of pulmonary fibrosis. *J Clin Invest* 1999;104:13–19.
15. Hagimoto N, Kuwano K, Inoshima I, Yoshimi M, Nakamura N, Fujita M, Maeyama T, Hara N. TGF-beta 1 as an enhancer of Fas-mediated apoptosis of lung epithelial cells. *J Immunol* 2002;168:6470–6478.
16. Sisson TH, Mendez M, Choi K, Subbotina N, Courey A, Cunningham A, Dave A, Engelhardt JF, Liu X, White ES, *et al.* Targeted injury of type II alveolar epithelial cells induces pulmonary fibrosis. *Am J Respir Crit Care Med* 2010;181:254–263.
17. Korfei M, Ruppert C, Mahavadi P, Henneke I, Markart P, Koch M, Lang G, Fink L, Bohle RM, Seeger W, *et al.* Epithelial endoplasmic reticulum stress and apoptosis in sporadic idiopathic pulmonary fibrosis. *Am J Respir Crit Care Med* 2008;178:838–846.
18. Young LR, Pasula R, Gulleman PM, Deutsch GH, McCormack FX. Susceptibility of Hermansky-Pudlak mice to bleomycin-induced type II cell apoptosis and fibrosis. *Am J Respir Cell Mol Biol* 2007;37:67–74.
19. Rouhani FN, Brantly ML, Markello TC, Helip-Wooley A, O'Brien K, Hess R, Huizing M, Gahl WA, Gochuico BR. Alveolar macrophage dysregulation in Hermansky-Pudlak syndrome type 1. *Am J Respir Crit Care Med* 2009;180:1114–1121.
20. Young LR, Borchers MT, Allen HL, Gibbons RS, McCormack FX. Lung-restricted macrophage activation in the pearl mouse model of Hermansky-Pudlak syndrome. *J Immunol* 2006;176:4361–4368.
21. Atochina-Vasserman EN, Bates SR, Zhang P, Abramova H, Zhang Z, Gonzales L, Tao JQ, Gochuico BR, Gahl W, Guo CJ, *et al.* Early alveolar epithelial dysfunction promotes lung inflammation in a mouse model of Hermansky-Pudlak syndrome. *Am J Respir Crit Care Med* 2011;184:449–458.
22. Guttentag SH, Akhtar A, Tao JQ, Atochina E, Rusiniak ME, Swank RT, Bates SR. Defective surfactant secretion in a mouse model of Hermansky-Pudlak syndrome. *Am J Respir Cell Mol Biol* 2005;33:14–21.
23. Mahavadi P, Korfei M, Henneke I, Liebisch G, Schmitz G, Gochuico BR, Markart P, Bellusci S, Seeger W, Ruppert C, *et al.* Epithelial stress and apoptosis underlie Hermansky-Pudlak syndrome-associated interstitial pneumonia. *Am J Respir Crit Care Med* 2010;182:207–219.
24. McGarry MP, Reddington M, Novak EK, Swank RT. Survival and lung pathology of mouse models of Hermansky-Pudlak syndrome and Chediak-Higashi syndrome. *Proc Soc Exp Biol Med* 1999;220:162–168.
25. Yoshioka Y, Kumasaka T, Ishidoh K, Kominami E, Mitani K, Hosokawa Y, Fukuchi Y. Inflammatory response and cathepsins in silica-exposed Hermansky-Pudlak syndrome model pale ear mice. *Pathol Int* 2004;54:322–331.
26. Peden AA, Rudge RE, Lui WW, Robinson MS. Assembly and function of AP-3 complexes in cells expressing mutant subunits. *J Cell Biol* 2002;156:327–336.
27. Feng L, Seymour AB, Jiang S, To A, Peden AA, Novak EK, Zhen L, Rusiniak ME, Eicher EM, Robinson MS, *et al.* The beta3A subunit gene (Ap3b1) of the AP-3 adaptor complex is altered in the mouse hypopigmentation mutant pearl, a model for Hermansky-Pudlak syndrome and night blindness. *Hum Mol Genet* 1999;8:323–330.
28. Zhen L, Jiang S, Feng L, Bright NA, Peden AA, Seymour AB, Novak EK, Elliott R, Gorin MB, Robinson MS, *et al.* Abnormal expression and subcellular distribution of subunit proteins of the AP-3 adaptor complex lead to platelet storage pool deficiency in the pearl mouse. *Blood* 1999;94:146–155.
29. Dell'Angelica EC, Shotelersuk V, Aguilar RC, Gahl WA, Bonifacino JS. Altered trafficking of lysosomal proteins in Hermansky-Pudlak syndrome due to mutations in the beta 3A subunit of the AP-3 adaptor. *Mol Cell* 1999;3:11–21.
30. Young LR, Gulleman PM, Deutsch GH, Weaver TE, McCormack FX. Bleomycin-induced fibrotic susceptibility of Hermansky-Pudlak syndrome (HPS) mice correlates with HPS genotypes associated with pulmonary fibrosis in humans [abstract]. *Am J Respir Crit Care Med* 2009;179:A3556.
31. Young LR, Gulleman PM, McCormack FX. Transgenic correction and bone marrow transplantation implicate epithelial protein mis-trafficking in constitutive alveolar macrophage activation in Hermansky-Pudlak mice [abstract]. *Am J Respir Crit Care Med* 2010;181:A1297.
32. Gulleman PM, Bridges JP, McCormack FX, Young LR. Susceptibility to alveolar type II cell apoptosis and pulmonary fibrosis in naturally occurring Hermansky Pudlak syndrome mice is not associated with endoplasmic reticulum stress [abstract]. *Am J Respir Crit Care Med* 2011;183:A5991.

33. Feng L, Rigatti BW, Novak EK, Gorin MB, Swank RT. Genomic structure of the mouse Ap3b1 gene in normal and pearl mice. *Genomics* 2000;69:370–379.
34. Yang W, Li C, Ward DM, Kaplan J, Mansour SL. Defective organellar membrane protein trafficking in Ap3b1-deficient cells. *J Cell Sci* 2000; 113:4077–4086.
35. Rice WR, Conkright JJ, Na CL, Ikegami M, Shannon JM, Weaver TE. Maintenance of the mouse type II cell phenotype in vitro. *Am J Physiol Lung Cell Mol Physiol* 2002;283:L256–L264.
36. Matute-Bello G, Lee JS, Frevert CW, Liles WC, Sutlief S, Ballman K, Wong V, Selk A, Martin TR. Optimal timing to repopulation of resident alveolar macrophages with donor cells following total body irradiation and bone marrow transplantation in mice. *J Immunol Methods* 2004;292:25–34.
37. Peden AA, Oorschot V, Hesser BA, Austin CD, Scheller RH, Klumperman J. Localization of the AP-3 adaptor complex defines a novel endosomal exit site for lysosomal membrane proteins. *J Cell Biol* 2004;164:1065–1076.
38. Dell'Angelica EC, Aguilar RC, Wolins N, Hazelwood S, Gahl WA, Bonifacino JS. Molecular characterization of the protein encoded by the Hermansky-Pudlak syndrome type 1 gene. *J Biol Chem* 2000;275: 1300–1306.
39. Moore BB, Hogaboam CM. Murine models of pulmonary fibrosis. *Am J Physiol Lung Cell Mol Physiol* 2008;294:L152–L160.
40. Liebler JM, Lutzko C, Banfalvi A, Senadheera D, Aghamohammadi N, Crandall ED, Borok Z. Retention of human bone marrow-derived cells in murine lungs following bleomycin-induced lung injury. *Am J Physiol Lung Cell Mol Physiol* 2008;295:L285–L292.
41. Rojas M, Xu J, Woods CR, Mora AL, Spears W, Roman J, Brigham KL. Bone marrow-derived mesenchymal stem cells in repair of the injured lung. *Am J Respir Cell Mol Biol* 2005;33:145–152.
42. Hashimoto N, Jin H, Liu T, Chensue SW, Phan SH. Bone marrow-derived progenitor cells in pulmonary fibrosis. *J Clin Invest* 2004; 113:243–252.
43. Ortiz LA, Gambelli F, McBride C, Gaupp D, Baddoo M, Kaminski N, Phinney DG. Mesenchymal stem cell engraftment in lung is enhanced in response to bleomycin exposure and ameliorates its fibrotic effects. *Proc Natl Acad Sci USA* 2003;100:8407–8411.
44. Glasser SW, Korfhagen TR, Wert SE, Bruno MD, McWilliams KM, Vorbroker DK, Whitsett JA. Genetic element from human surfactant protein SP-C gene confers bronchiolar-alveolar cell specificity in transgenic mice. *Am J Physiol* 1991;261:L349–L356.
45. Hardie WD, Kerlakian CB, Bruno MD, Huelsman KM, Wert SE, Glasser SW, Whitsett JA, Korfhagen TR. Reversal of lung lesions in transgenic transforming growth factor alpha mice by expression of mutant epidermal growth factor receptor. *Am J Respir Cell Mol Biol* 1996;15:499–508.
46. Mishra A, Weaver TE, Beck DC, Rothenberg ME. Interleukin-5-mediated allergic airway inflammation inhibits the human surfactant protein c promoter in transgenic mice. *J Biol Chem* 2001;276:8453–8459.
47. Bridges JP, Xu Y, Na CL, Wong HR, Weaver TE. Adaptation and increased susceptibility to infection associated with constitutive expression of misfolded SP-C. *J Cell Biol* 2006;172:395–407.
48. Lawson WE, Cheng DS, Degryse AL, Tanjore H, Polosukhin VV, Xu XC, Newcomb DC, Jones BR, Roldan J, Lane KB, *et al*. Endoplasmic reticulum stress enhances fibrotic remodeling in the lungs. *Proc Natl Acad Sci USA* 2011;108:10562–10567.
49. Maitra M, Wang Y, Gerard RD, Mendelson CR, Garcia CK. Surfactant protein A2 mutations associated with pulmonary fibrosis lead to protein instability and endoplasmic reticulum stress. *J Biol Chem* 2010;285:22103–22113.